Natural Resources Canada
Ressources naturelles Canada

Preliminary results of shallow subsurface geological mapping, Sabine Peninsula, western Arctic Islands

V.I. Brake, M.J. Duchesne, and T.A. Brent

Geological Survey of Canada
Current Research 2012-5

2012

Canada

Geological Survey of Canada
Current Research 2011-5

Preliminary results of shallow subsurface geological mapping, Sabine Peninsula, western Arctic Islands

V.I. Brake, M.J. Duchesne, and T.A. Brent

2012

©Her Majesty the Queen in Right of Canada 2012

ISSN 1701-4387
Catalogue No. M44-2012/5E-PDF
ISBN 978-1-100-20040-8
doi: 10.4095/289712

A copy of this publication is also available for reference in depository libraries across Canada through access to the Depository Services Program's Web site at http://dsp-psd.pwgsc.gc.ca

A free digital download of this publication is available from GeoPub: http://geopub.nrcan.gc.ca/index_e.php

Toll-free (Canada and U.S.A.): 1-888-252-4301

Recommended citation

Brake, V.I., Duchesne, M.J., and Brent, T.A., 2012. Preliminary results of shallow subsurface geological mapping, Sabine Peninsula, western Arctic Islands; Geological Survey of Canada, Current Research 2012-5, 13 p. doi:10.4095/289712

Critical review

A. Embry

Authors

V.I. Brake (Virginia.Brake@RNCan-NRCan.gc.ca)
M.J. Duchesne (Mathieu.Duchesne@RNCan-NRCan.gc.ca)
Geological Survey of Canada
490, rue de la Couronne
Québec, Quebec
G1K 9A9

T.A. Brent (Tom.Brent@NRCan-RNCan.gc.ca)
Geological Survey of Canada
3303-33 Street NW
Calgary, Alberta
T2L 2A7

Correction date:

All requests for permission to reproduce this work, in whole or in part, for purposes of commercial use, resale, or redistribution shall be addressed to: Earth Sciences Sector Copyright Information Officer, Room 650, 615 Booth Street, Ottawa, Ontario K1A 0E9.
E-mail: ESSCopyright@NRCan.gc.ca

Preliminary results of shallow subsurface geological mapping, Sabine Peninsula, western Arctic Islands

V.I. Brake, M.J. Duchesne, and T.A. Brent

Brake, V.I., Duchesne, M.J., and Brent, T.A., 2012. Preliminary results of shallow subsurface geological mapping, Sabine Peninsula, western Arctic Islands; Geological Survey of Canada, Current Research 2012-5, 13 p doi:10.4095/289712

Abstract: The study of the Sabine Peninsula, western Arctic Islands, was undertaken as part of the Government of Canada's Geo-mapping for Energy and Minerals (GEM) program. Given the cost of data acquisition in frontier areas, vintage data sets still possess a strong value. This study utilizes modern geoscientific processing and interpretation methods applied to a suite of data collected during the initial round of exploration that took place between the late 1960s and early 1980s. The focus of this project is to map the subsurface of Sabine Peninsula and provide a more detailed seismic stratigraphy to ultimately develop play concepts that were not identified during the initial round of exploration.

Following the reprocessing of the seismic data sets, six time-structure maps of the Triassic through Cretaceous succession of the Sverdrup Basin (<3 s) display changes in the morphology of the horizons throughout the Mesozoic. Several features are preserved throughout the Mesozoic section, for instance, the presence of a linear flexure inherited from the deeper section (possibly Permian) indicates the location of a possible paleoshelf edge. Additionally, the presence of a depression, and the gradual infill of that depression provide clues as to what type of seismic successions can be expected in the deeper section and the adjacent offshore.

Résumé : L'étude de la péninsule Sabine, dans l'ouest de l'archipel Arctique, a été entreprise dans le cadre du programme « Géocartographie de l'énergie et des minéraux » (GEM) du gouvernement du Canada. Compte tenu des coûts d'acquisition des données dans les régions pionnières, les jeux de données anciens ont encore une grande valeur. Cette étude utilise des méthodes géoscientifiques modernes pour le traitement et l'interprétation d'une série de données acquises lors de la phase initiale d'exploration qui a eu lieu entre la fin des années 1960 et le début des années 1980. L'objectif du projet consiste à cartographier la subsurface de la péninsule Sabine et à établir une sismostratigraphie plus détaillée pour éventuellement mettre en valeur des zones pétrolières qui n'avaient pas été décelées lors de la phase initiale d'exploration.

Après un nouveau traitement des jeux de données sismiques, six cartes structurales ont été créées à partir des temps de parcours pour représenter la succession du bassin de Sverdrup, du Trias au Crétacé (< 3 s). Ces cartes montrent des changements dans la morphologie des horizons tout au long du Mésozoïque. Plusieurs attributs sont conservés dans l'ensemble de la coupe du Mésozoïque; notamment, la présence d'une flexure linéaire héritée de couches plus en profondeur (possiblement dans le Permien) indique l'emplacement de ce qui serait vraisemblablement la bordure d'une ancienne plate-forme. En outre, la présence d'une dépression graduellement remplie fournit des indications sur le type de successions sismiques que l'on peut s'attendre à trouver plus en profondeur et dans la zone extracôtière adjacente.

INTRODUCTION

The Sabine Peninsula of Melville Island is located on the fringe of the Sverdrup Basin in the Queen Elizabeth Islands of the western Arctic (Fig. 1). The earliest geological observations of Melville Island date back to 1819 when the island was discovered by Europeans (Harrison, 1995). Many subsequent geological and structural observations were made during periodic visits to the island. By 1950, two aerial photographic studies were completed (Greenaway and Colthorpe, 1948; Dunbar and Greenaway, 1956), indicating the presence of a major fold belt (Harrison, 1995). The age and timing of the fold belt as well as the potential for hydrocarbon deposits sparked the interest of researchers and companies alike. Several petroleum companies were exploring the hydrocarbon potential during the 1960s and the first well was drilled in 1961 near Winter Harbour by Dome Exploration as the main operator. Panarctic Oils Ltd. was formed in 1967, as an initiative by the Canadian Government to promote exploration in the Canadian Arctic. The Panarctic Oils Ltd. partnership consolidated the interests of those companies and individuals with land holdings with the government acting as a major shareholder. In total, 52 wells were drilled on Melville Island and its surrounding waters during the 1961–1985 exploration boom — 22 of which were acquired on the Sabine Peninsula. The collection of more than 3400 line-kilometres of seismic-reflection data, later used along with gravity and magnetic data as well as the well data allowed petroleum companies to evaluate the resource potential. Three separate gas fields were discovered by Panarctic Oils Ltd. in the vicinity of the northern Sabine Peninsula: Drake Point, Hecla, and Roche Point. Feasibility studies for the development of the gas fields were conducted early in the 1980s, however the fall of world gas prices in the mid-1980s combined with an abundant gas market led to the reduced interest on Melville Island and the Arctic in general (Harrison, 1995).

GEOLOGICAL SETTING

The Sverdrup Basin of the western Arctic Islands spans 1000 km from Prince Patrick Island to Ellesmere Island and measures as much as 350 km in width, containing a

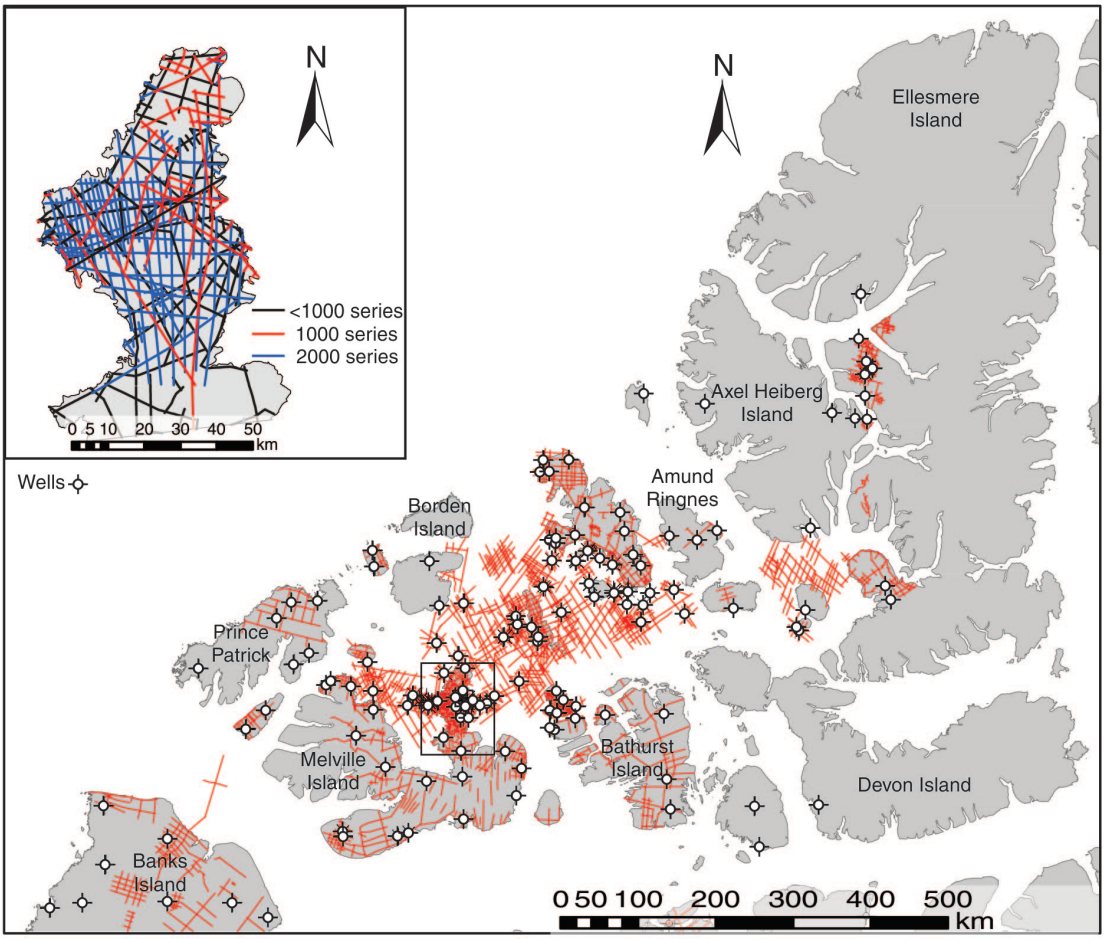

Figure 1. Distribution of seismic and well-data coverage in the Canadian western Arctic. The inset of Sabine Peninsula indicates the difference in data coverage among the data series investigated.

thickness of strata greater than 13 km, with a distinct shelf to deep basin topography (Embry and Beauchamp, 2008). The Sverdrup Basin unconformably overlies the deformed rocks of the Franklinian Basin, however the Franklinian succession was superseded by widespread rifting following the Late Devonian–earliest Carboniferous Ellesmerian Orogeny. The resultant structural depression acted as a major depocentre from the Carboniferous through the Paleogene (Embry and Beauchamp, 2008).

The strata of Melville Island can broadly be grouped into three sedimentary successions, as summarized by Goodbody and Christie (1993): 1) the upper Precambrian to Upper Devonian deformed strata of the Franklinian Basin, 2) Pennsylvanian to early Tertiary strata of the Sverdrup Basin, and 3) Upper Tertiary and younger – probably Pliocene-Miocene Beaufort Formation. The Beaufort Formation is absent on the Sabine Peninsula and scarce across the remainder of Melville Island, thus, only the Franklinian and Sverdrup successions will be discussed.

The Sverdrup and Franklinian successions are separated by a sub-Carboniferous unconformity. This formed during the Ellesmerian Orogeny, which led to widespread re-organization in the western Arctic Islands. The Franklinian succession consists of shale, sandstone, bioturbated and locally fossiliferous carbonate, and chert, as well as gypsum and halite (Dewing and Embry, 2007). Similarly, the Sverdrup succession is dominated by shale, chert, carbonate, and olistostromes interfingered with sandstone units. Also present are minor amounts of bioturbated and locally fossiliferous carbonate, gypsum, halite, chert, and igneous rocks (Dewing and Embry, 2007). The axis of the Sverdrup Basin was located north of the present-day Melville Island at the basin margin; consequently sedimentary units are thicker basinward or on the northern Sabine Peninsula (Goodbody and Christie, 1993).

Only a small portion of the outcropping bedrock on Melville Island is part of the Sverdrup Basin. These occur on Sabine Peninsula, as well as Sproule Peninsula and Cape Grassy areas. The remainder of the island consists of the deformed rocks of the Franklinian Basin. Within the study area strata of the Franklinian Basin is present solely in the subsurface.

The Sverdrup succession was affected by the Eurekan Orogeny early in the Cenozoic and consequently much of the Paleogene and Neogene succession is absent. The geology of the Sabine Peninsula consists of slightly deformed Triassic to Quaternary sandstone, siltstone, shale, and minor amounts of carbonate. Additionally, evaporitic rocks are exposed in two piercement diapirs on northern Sabine Peninsula – the Barrow and Colquhoun domes, which consist of deformed anhydrite and gypsum. Furthermore, halite is believed to be present beneath the domes, given the presence of halite elsewhere within the Sverdurp Basin (Harrison, 1995). The underlying halite did not pierce the anhydrite; instead the anhydrite is believed to have acted as a diapiric material (Stephenson et al., 1992)

The strata of the Sverdrup Basin succession on Melville Island are affected by a series of folds including the Murray Harbour syncline in the north of the peninsula and the Drake Point anticline and the Marryatt Point syncline to the south. The timing of folding is proposed to be Eurekan (Waylett, 1990; Harrison, 1995); however, regional stratigraphic studies indicate that the structures are pre-Eurekan, given that the maximum burial occurred prior to the Eurekan Orogeny and the time of hydrocarbon generation (Dewing and Obermajer, 2011).

On average, the wells located on Sabine Peninsula penetrate more than 2600 m of the Permian through to Cretaceous stratigraphy. The deepest well drilled on the Sabine Peninsula is Panarctic Oil Ltd.'s Marryatt K-71 drilled to a depth of 5467 m in 1982. In contrast, the well penetrating the oldest strata on Sabine Peninsula, Eldridge Bay E-79, was drilled by Panarctic Oil Ltd. in 1973 to a depth of 3049 m and sampled early Triassic through mid-Ordovician stratigraphy. This stratigraphy, however, is not typical for the entire peninsula.

The Sabine Peninsula represents the area of the western Arctic with the highest density of seismic coverage (Fig. 1). More than 3400 km of 2-D seismic-reflection data cover the onshore area of Sabine Peninsula. This network of seismic lines tends to cross and intersect covering a time-depth of as much as 8 s. The data coverage, however, as well as the quality of data are variable (Fig. 1, inset). Two obvious gaps in seismic coverage, and consequently gaps on the resultant time-structure maps, occur in the northern area of Sabine Peninsula and represent the presence of the Barrow and Colquhoun domes. Seismic data can be grouped into three distinct data series based on acquisition parameters: the less than 1000-series, 1000-series, and 2000-series lines. The less than 1000-series and 1000-series lines are present across most of the Sabine Peninsula. In comparison, the 2000-series lines are mainly located south of Barrow Dome. The less than 1000-series lines are the generally the poorest quality lines, whereas the 2000-series lines are the best quality data available.

SEISMIC DATA SET AND PROCESSING

Data access has been obtained through a Memorandum of Understanding (MOU) between the Geological Survey of Canada (GSC), Panarctic Oils Ltd., the Arctic Islands Exploration Group, and the Offshore Arctic Exploration Group joint ventures parties signed in 1997. On Sabine Peninsula, the data set consists of original land seismic-field tapes transcribed from 21-, 7-, and 9-track media to different digital Society of Exploration Geophysicists (SEG)

file formats. Data were collected using a dynamite charge of 20 kg per shot to 30 kg per shot at about 20 m below the surface. Shot-point spacing was greatly variable ranging from 300 m to 67 m, the latter spacing being used for most surveys. The majority of the acquisition campaigns were recorded using 48- and 96-channel systems. Channel stations were generally deployed using 9 receivers distant of about 8 m and channel interval varied from 50 m to 70 m. The common-midpoint multiplicity of the data set is mostly low, ranging from single to 12-fold coverage. Recording length is on average 6 s, but some lines have been recorded on 9 s.

Data artifacts are grouped into two different noise categories: coherent and random. Coherent noise possesses a systematic phase relation between adjacent traces. This type of noise is generally distributed according to repetitive patterns along a seismic section. Permafrost or ice breaks are typical coherent artifacts recorded on the western Arctic Island data set that are caused by the fracturing of the permafrost triggered by the energy of the shot (Merritt, 1974). Acquisition footprints are another coherent noise observed on the data (Fig. 2b). They possess a 'criss-cross' signature attributed to the geometric distribution of shot and receiver stations at the surface (Marfurt et al., 1998). Random noise is attributed to energy that does not correlate in the time versus distance space between adjacent traces. Local changes in the frequency content are one type of random noise caused by both the occurrence of permafrost and variations of its physical properties on land as well as transition zones (i.e. land to sea ice acquisition areas) (Brent, 2006). An additional type of random noise is inconsistent amplitude and frequency scaling of adjacent traces induced by transcription of original seismic field tapes to digital SEG file formats.

Permafrost breaks and acquisition footprints have been successfully attenuated by carefully designing frequency-wavenumber (FK) filters based on the approximate seismic velocity of the direct arrival of the permafrost and the acquisition geometry parameters of each survey (Fig. 2a, b). A frequency-distance (FX) random-noise prediction filter permitted to eliminate most of the random noise that contaminated the stacked sections (Canales, 1984). Then, seismic data have been migrated using a windowed Kirchhoff post-stack time migration to collapse diffraction hyperbolae located at various time-depths (Fig. 2a). This method decomposes the initial seismic image into different time windows for which different angle and aperture parameters and percentages of the root-mean squared velocity field are used before reconstructing the image. A time-variant Ormsby filter is subsequently used to attenuate remaining high and low frequency noise present on the original stacked sections or induced by the different processing steps. Finally, amplitudes are balanced using a residual gain curve that allows compensating for attenuation and changes in wavelet frequency content without downweighting the strong seismic events.

Synthetic seismograms were used to optimize seismic-to-well ties (Fig. 3). Synthetic seismograms result from the computation of a reflection-coefficient series obtained by the product of velocity and density logs that is later convolved with a seismic wavelet (Sengbush et al., 1961; Lindseth, 1979). In this study, reflection-coefficient series were convolved with a seismic wavelet modelled from frequency matching (Matheney and Nowack, 1995). In this method, a zero-phase wavelet is first modelled from the average of the frequency spectra of a number of traces calculated over a fixed time window. To be representative of the seismic impulsion, the wavelet was modelled using 50 traces located on both sides of the well that were extracted from the seismic section crossing the well.

SEISMIC VISUALIZATION AND INTERPRETATION METHODS

Reprocessed SEG-y files were loaded into IHS-Seismic Micro-Technology's (SMT) Kingdom seismic data visualization and interpretation software. Lines were quality controlled within this software to ensure consistency and selected lines bulk shifted or phase rotated as needed.

First, key reflections were identified and their seismic horizons were traced laterally based the coherency of the reflection along distance or until the seismic resolution allowed (Fig. 4). Reflections were picked starting with what was considered to be the best quality seismic lines — those of the 2000-series, in the area with the closest line spacing — the west side of Sabine Peninsula near the Panarctic Oils Ltd. et al. well Chads Creek B-64. Key horizons were picked semi-automatically and edited manually on the seismic sections. Seed points were generated where seismic traces on crossline overlap, permitting the horizons to be correlated with adjacent lines. Then, grids were created from the picked horizons.

The interpreted horizons were chosen based on their position within the succession as well as their amplitude and continuity. Regional well data, including available age control, lithology, and a suite of log data were correlated with seismic profiles with synthetic seismograms (Fig. 3).

The reliability of an output grid as a function of the seismic coverage density was considered prior to the calculation of the time-structure maps. The density of the seismic coverage was calculated by dividing the Sabine Peninsula into three areas: an area in the north with lines spaced several kilometres apart, another in the central part of the peninsula where the landmass is widest and covered by the highest density of seismic lines, and finally an area in the south near the southern limit of the study area with moderate seismic coverage (Fig. 5a). The resultant calculations indicate that the seismic coverage for Sabine Peninsula is 0.87 line-kilometres of seismic per square kilometre. The northern area of the peninsula had an average seismic coverage of

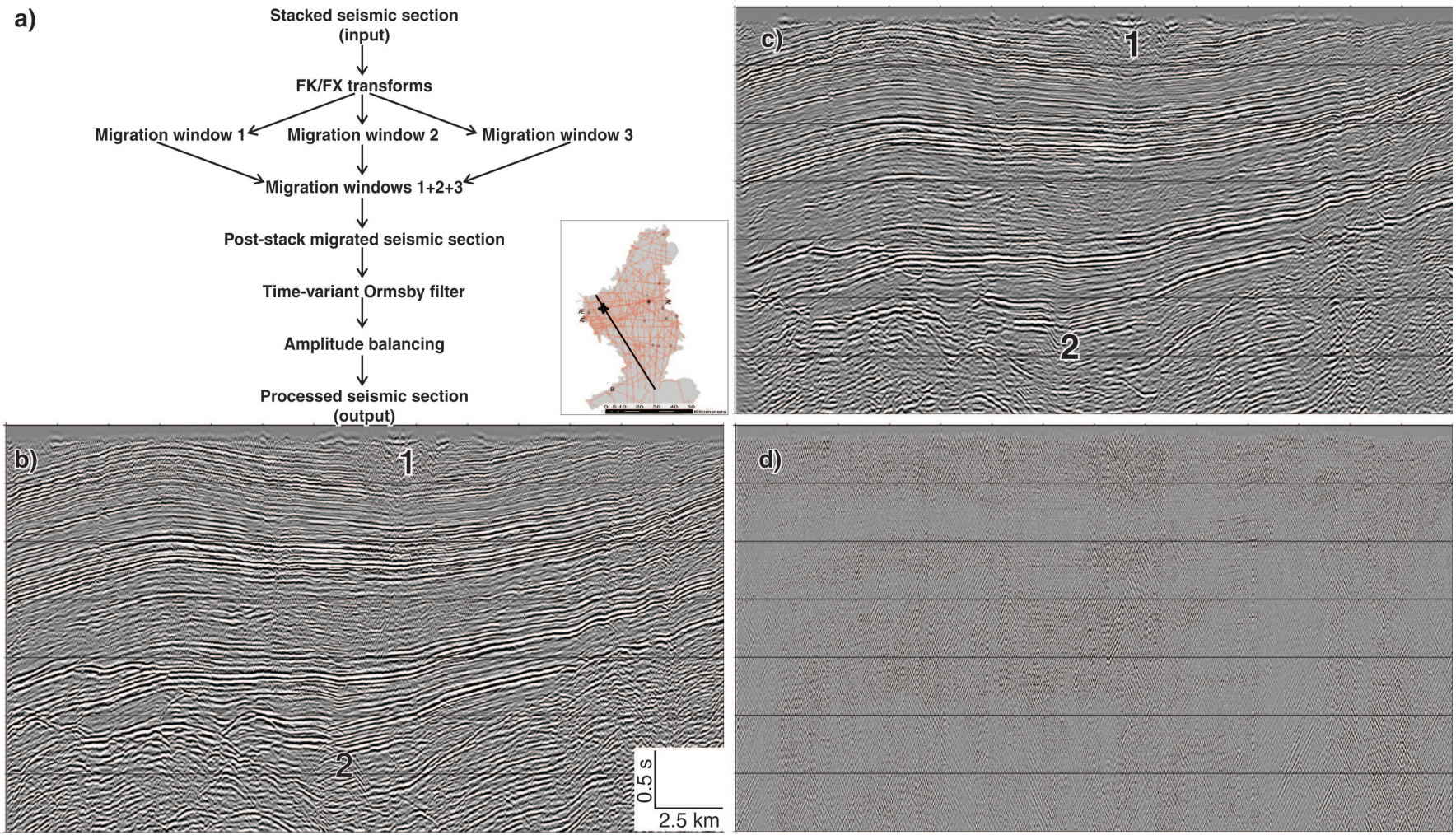

Figure 2. **a)** Processing flow utilized on a case-by-case basis for seismic lines on the Sabine Peninsula. **b)** Original stacked section 1920, **c)** reprocessed section 1920, and **d)** difference plot of Figure 2b minus Figure 2c, showing the distribution of the noise removed using the processing flow presented in Figure 2a. The reprocessing permitted to successfully attenuate acquisition footprints (1) and collapse diffraction hyperbolae (2).

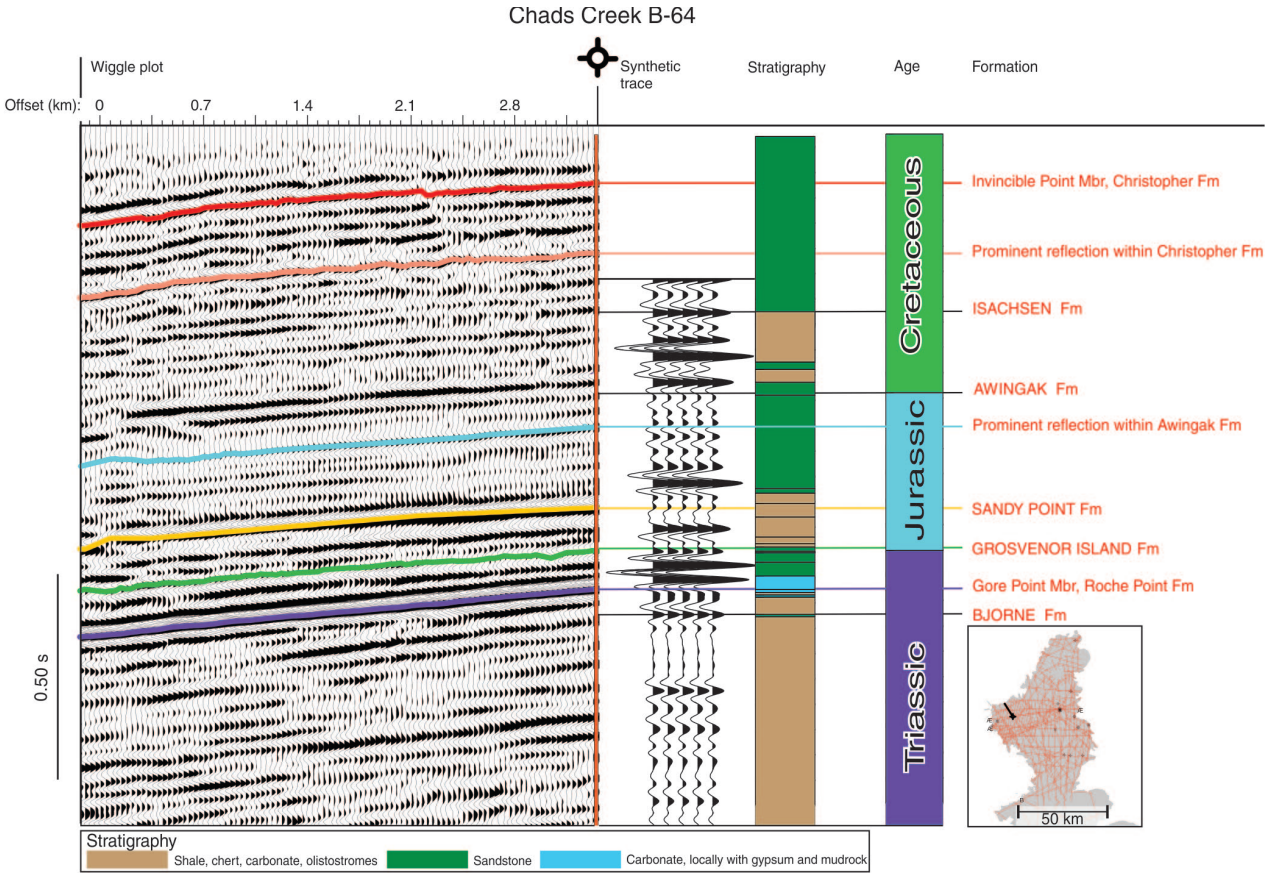

Figure 3. Comparison of the wiggle plot, synthetic trace, stratigraphy, age, and formation tops for the Chads Creek B-64 well. Stratigraphy, age, and formation tops are based up on Dewing and Embry (2007).

0.71 line-kilometres of seismic per square kilometre, whereas the central and southern areas of the peninsula have values of 1.36 line-kilometres of seismic per square kilometre and 0.54 line-kilometres of seismic per square kilometre, respectively. As a result, a higher degree of confidence is attributed to the central part of the grids.

Time-structure maps of the key horizons were computed by a universal kriging algorithm. Kriging methods allow the interpolation of values of a random field at unobserved locations by a distance-weighted approach. One of the main assumptions made in kriging is that the estimated data are stationary, i.e. the average of a scattered point set is constant from one region to another. When a spatial trend exists in a random field the stationary assumption is violated. Since all picked horizons showed a strong linear trend for time-depth over distance, universal kriging was used to grid that data (Fig. 5b). Universal kriging permits the interpolation of a nonstationary random field by adding a term in the kriging equation that accommodates any linear trends present in a scattered point set (Chilès and Delfiner, 1999).

RESULTS

Seismic stratigraphy

The shallow succession consists of stacked, parallel, semicontinuous to chaotic seismic reflections with an overall draped morphology. The distribution of the reflections and consequently the distribution of the seismic units that make up the succession are variable across Sabine Peninsula. The shallow seismic succession can be grouped into five distinct reflection units separated by the interpreted surfaces.

Interpreted surfaces

Gore Point Member, Roche Point Formation

The Gore Point reflection represents the deepest, and hence, oldest reflection correlated across the Sabine Peninsula within the scope of this study (Fig. 4). The reflection was ubiquitous across the entire peninsula and readily identifiable

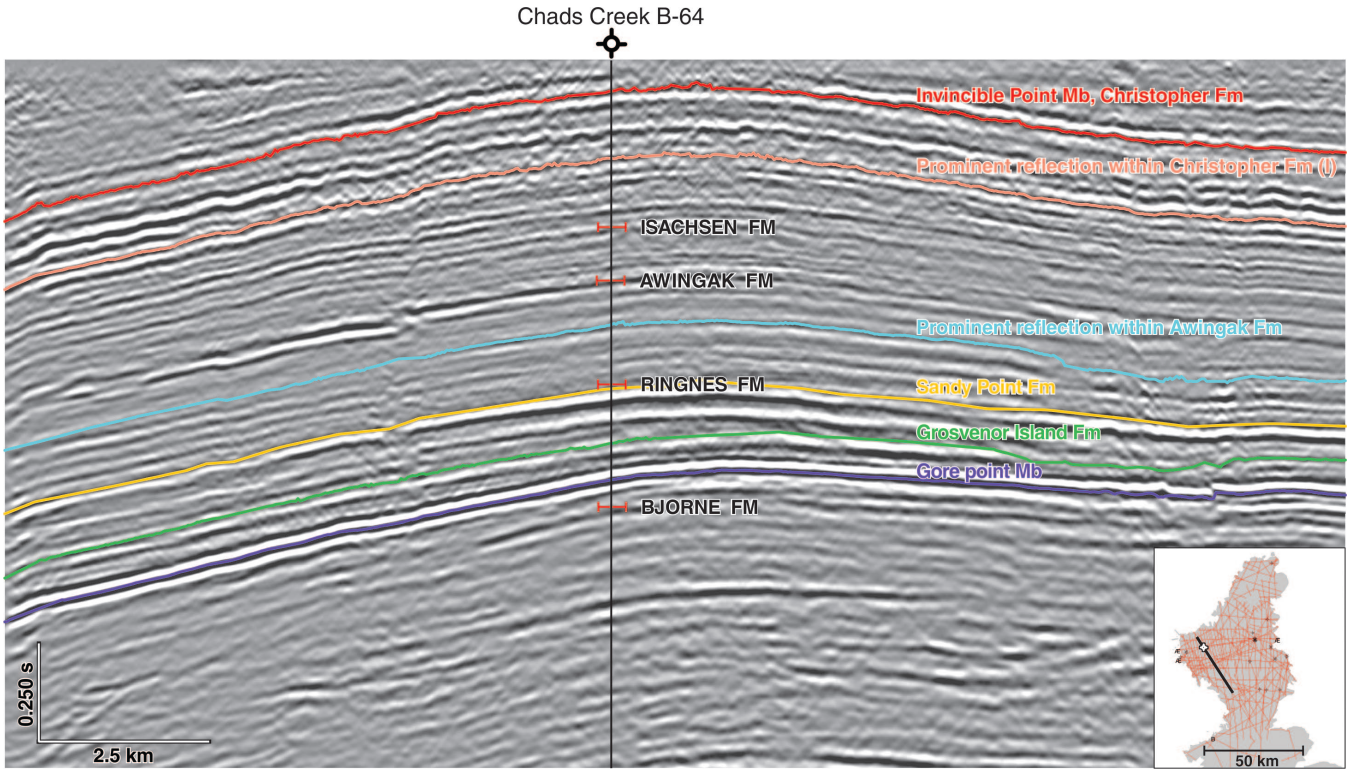

Figure 4. Seismic-stratigraphic interpretation using a reprocessed 1000-series line on Sabine Peninsula. Seismic-to-well ties incorporate formation top, well logs (gamma ray, calliper, delta time, spontaneous potential, etc.), and synthetic seismogram data (not shown on figure).

based on its high amplitude and continuous character. The amplitude is consistent across the peninsula and across data series, although the reflection does weaken slightly in the southern part of the peninsula where the reflection nears the surface. The reflection was selected and correlated based on its position within the stratigraphic succession and the fact that it separates the shallower, better imaged, relatively artifact-free section from the deeper section (i.e. below ~3 s). The reflection denotes the Gore Point Member of the Roche Point Formation, of the Schei Point Group, which consists predominantly of limestone with calcareous sandstone and siltstone (Embry, 1984a)

The Gore Point horizon was correlated along the entire length of a given seismic line with the exception of the southern extent of the peninsula near Eldridge Bay and Sherard Bay, where the horizon approached the surface.

Grosvenor Island Formation

The Grosvenor Island reflection is among the deepest reflections correlated across the Sabine Peninsula (Fig. 4). The amplitude of the reflection is not consistent and, in general, the reflection weakens toward the north. Overall, the reflection was easier to interpret on east-trending lines. The reflection was chosen based on its position within the deeper sequence. Formation-top data indicate that the reflection denotes the Grosvenor Island Formation. Accordingly, the lithology corresponds to marine to brackish shale and siltstone (Embry and Johannessen, 1992).

The Grosvenor Island horizon was correlated over much the same area as the Gore Point reflection with the exception of the southernmost extent of the study area where the horizon approached the surface. The Grosvenor Island horizon was difficult to interpret on the less than 1000-series lines and as a result was only correlated on a few lines of this series. On the other hand, the reflection was readily correlated on the 1000- and 2000-series lines.

Sandy Point Formation

The Sandy Point reflection, like the other reflections described thus far is located in the deeper section of the data set (Fig. 4). The amplitude of the reflection was variable across the data set with a further loss of amplitude in the vicinity of well F-16. Also, the amplitude of the reflection weakened as the reflection approached the surface in the southernmost extent of the study area. The reflection correlates with the Sandy Point Formation on available formation top data. The Sandy Point Formation consists of fine- to medium-grained sandstone, siltstone, and shale (Embry, 1984b).

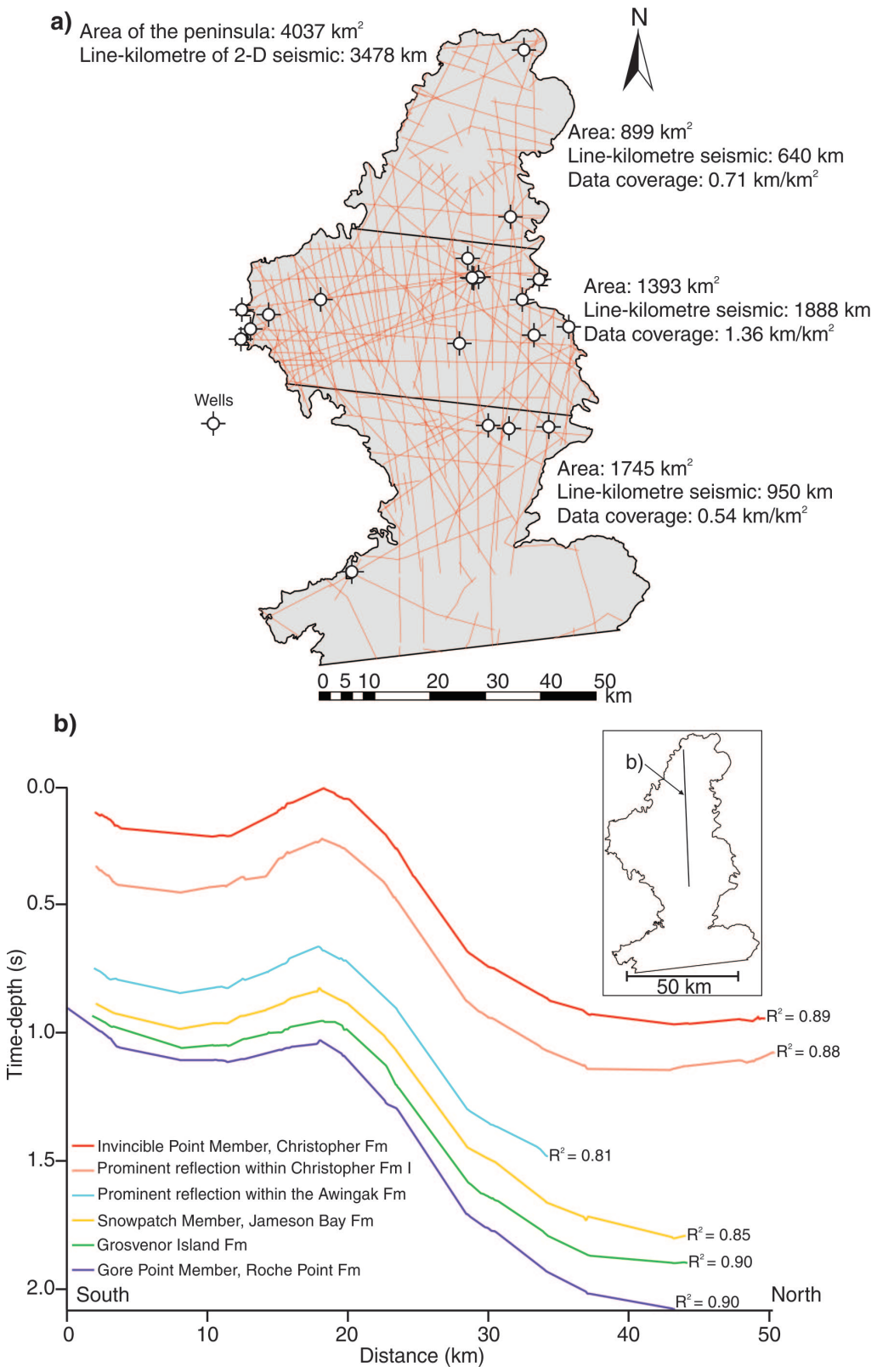

Figure 5. a) Density of seismic coverage for the Sabine Peninsula. **b)** Time-depth versus distance plot for seismic horizons picked along Sabine Peninsula. Linear correlation coefficient (R2) of each horizon is displayed on the plot.

The Sandy Point Formation was correlated over almost the exact same area as the Grosvenor Island horizon. Also similar to the Grosvenor Island horizon, the Sandy Point reflection was difficult to correlate on the less than 1000-series lines and consequently was interpreted only in the northeast section of the peninsula on this data series. The reflection was readily correlated on the 1000- and 2000-series lines.

Prominent reflection within the Awingak Formation

The prominent Awingak reflection is located approximately midway within the seismic interval investigated (Fig. 4). The high amplitude of the reflection appeared to be consistent on both the less than 1000- and 1000-series lines, yet was variable on the 2000-series lines. In general, the amplitude weakened toward the north and again where the reflection approaches the surface at the southernmost extent of the study area. When correlated with available formation-top data the reflection is located below the Awingak Formation and above the Ringnes Formation. The reflection is therefore determined to be a prominent reflection within the Awingak Formation. The Awingak Formation is composed of fine-grained quartzose sandstone, siltstone, and shale predominantly of marine origin (Harrison, 1995).

The coverage of the prominent Awingak horizon interpretation differs from the Sandy Point horizon in the northwest area of Sabine Peninsula. The correlation of the prominent Awingak horizon relies primarily on the 1000- and 2000-series lines.

Prominent reflection within the Christopher Formation I

The prominent reflection within the Christopher Formation I, is one of two prominent reflections investigated within the formation (Fig. 4). The reflection is located in the upper part of the investigated section. The reflection was generally of high amplitude and fairly easy to interpret although the reflection had a 'chattery', or broken-up appearance likely as a result of residual acquisition artifacts. Overall, it was easier to interpret east-trending lines rather than north-trending lines. According to available formation-top information the reflection consistently occurs between the Christopher Formation and the Walker Island Member, or the top of the Isachsen Formation, and is therefore referred to as "prominent reflection within the Christopher Formation". The Christopher Formation consists of mudrock, minor siltstone, and very fine-grained sandstone (Harrison, 1995).

This prominent reflection covered an area larger than that described for the preceding Sandy Point and Awingak horizons. In particular, the horizon was readily correlated on the less than 1000-series lines in the northern areas of the peninsula as well as on the 1000- and 2000-series lines.

Invincible Point Member, Christopher Formation

The Invincible Point reflection of the Christopher Formation is the shallowest reflection interpreted (Fig. 4). The reflection generally has high amplitude, although the amplitude is not always constant. Unlike the other reflections that weaken as they approach the surface, this reflection tends to maintain its high amplitude. The reflection can be traced on few less than 1000-series lines, however, it is readily identifiable on the 1000- and 2000-series lines. Similar to the preceding reflection within the Christopher Formation, the reflection has an irregular, broken-up appearance attributed to residual acquisition artifacts, therefore offsets are not evident and the reflection is interpreted despite any offset. Like the previous reflection, the reflection occurs between the Christopher Formation and the Walker Island Member of the Isachsen Formation. The reflection corresponds to the Invincible Point Member of the Christopher Formation. The Invincible Point Member was not recorded by Panarctic Oils Ltd., however, the type section was defined on Sabine Peninsula at the North Sabine H-49 well (A.F. Embry, pers. comm., 2011).

The Invincible Point reflection covers a smaller area then its predecessor. More specifically, the horizon approaches the surface not only in the southernmost area of data coverage, but in the east as well. The reflection is easily correlated on seismic lines of each line series.

FAULTING

Faulting is noted throughout the data set mainly in the form of extensional faults. The interval affected spans from below the Gore Point reflection to just below the Christopher Formation I reflection. Offset due to faulting is minor and generally on the order of 0.1 s. Reflections are readily identified across faults despite offset.

TIME-STRUCTURE MAPS

Given the fact that the subsurface sequence is generally flat, the time-structure maps are arranged in a stacked pattern. Overall, the maps display several similar trends; for instance, the shallowest part of the grids is in the southern part of the peninsula, the deepest areas are in the north. Also,

the southernmost extent of the grid coincides with where the reflection approaches the surface. Finally, the general grid morphology is similar for each grid, with several features inherited from the deeper subsurface structure.

Gore Point Member, Roche Point Formation

The Gore Point time-structure map spans a time-depth from 0.12 s in the near surface to 2.3 s (Fig. 6). The map reveals much about the subsurface structure of the Sabine Peninsula. Perhaps the most notable feature is the depression centred on the widest part of the peninsula. Another notable feature is the presence of the linear flexure spanning from Macdougall Point to Cape Caledonia.

Grosvenor Island Formation

The time-structure map of the Grosvenor Island horizon spans from a time-depth of 0.6 s to 2.07 s (Fig. 6). In comparison to the deeper Gore Point time-structure map the two maps are quite similar. Subtle changes are noted in the depression morphology, however, the linear flexure noted on the Gore Point map is maintained.

Sandy Point Formation

The Sandy Point time-structure map ranges in time-depth from 0.5 s to 1.9 s (Fig. 7). Similar to the previous two maps, subtle changes are noted in the morphology of the depression whereas the presence of the linear flexure is maintained.

Prominent reflection within the Awingak Formation

The Awingak time-structure map spans a time-depth of 0.2 s to 1.7 s (Fig. 7). The Awingak map indicates that the depression noted on the previous maps gradually becomes more isolated upward in the stratigraphy. The linear flexure, however, tends to maintain its position with some subtle differences.

Prominent reflection within the Christopher Formation I

The prominent reflection within the Christopher Formation I time-structure map ranges from nearly the surface to 1.3 s (Fig. 8). The depression that is noted on the maps ranging from Gore Point upward in the stratigraphy gradually becomes more and more isolated whereas the linear depression is maintained.

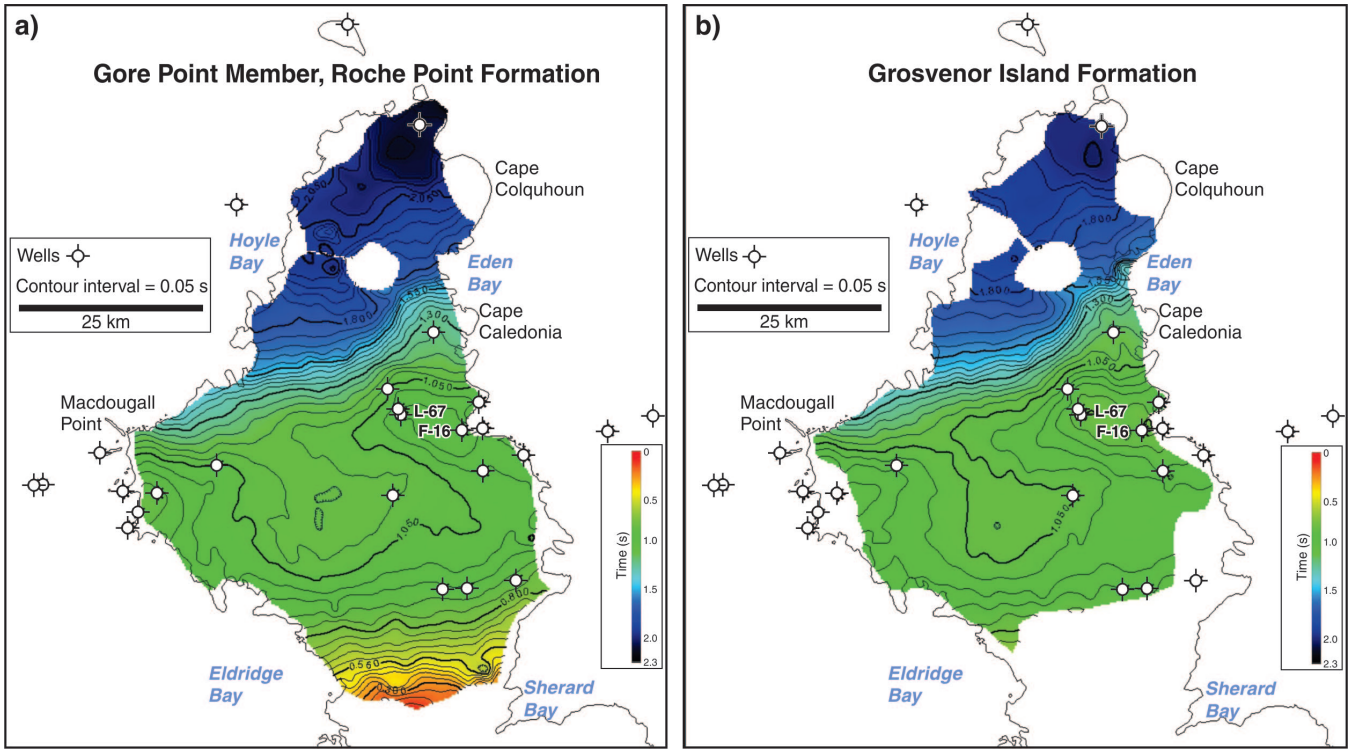

Figure 6. Time-structure maps of **a)** Gore Point Member (Roche Point Formation) and **b)** Grosvenor Island Formation reflections identified within the shallow subsurface of Sabine Peninsula.

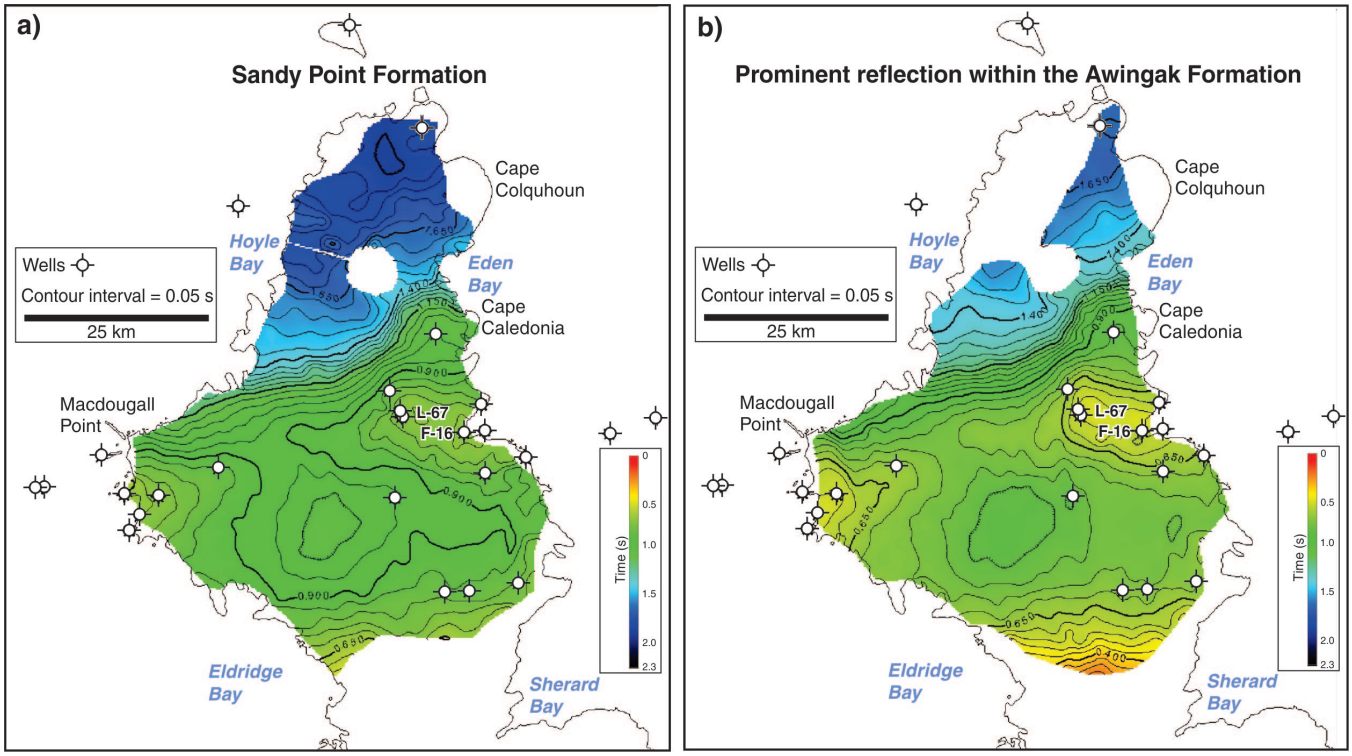

Figure 7. Time-structure maps of prominent reflection within the **a)** Sandy Point Formation and **b)** Awingak Formation reflection identified within the shallow subsurface of Sabine Peninsula.

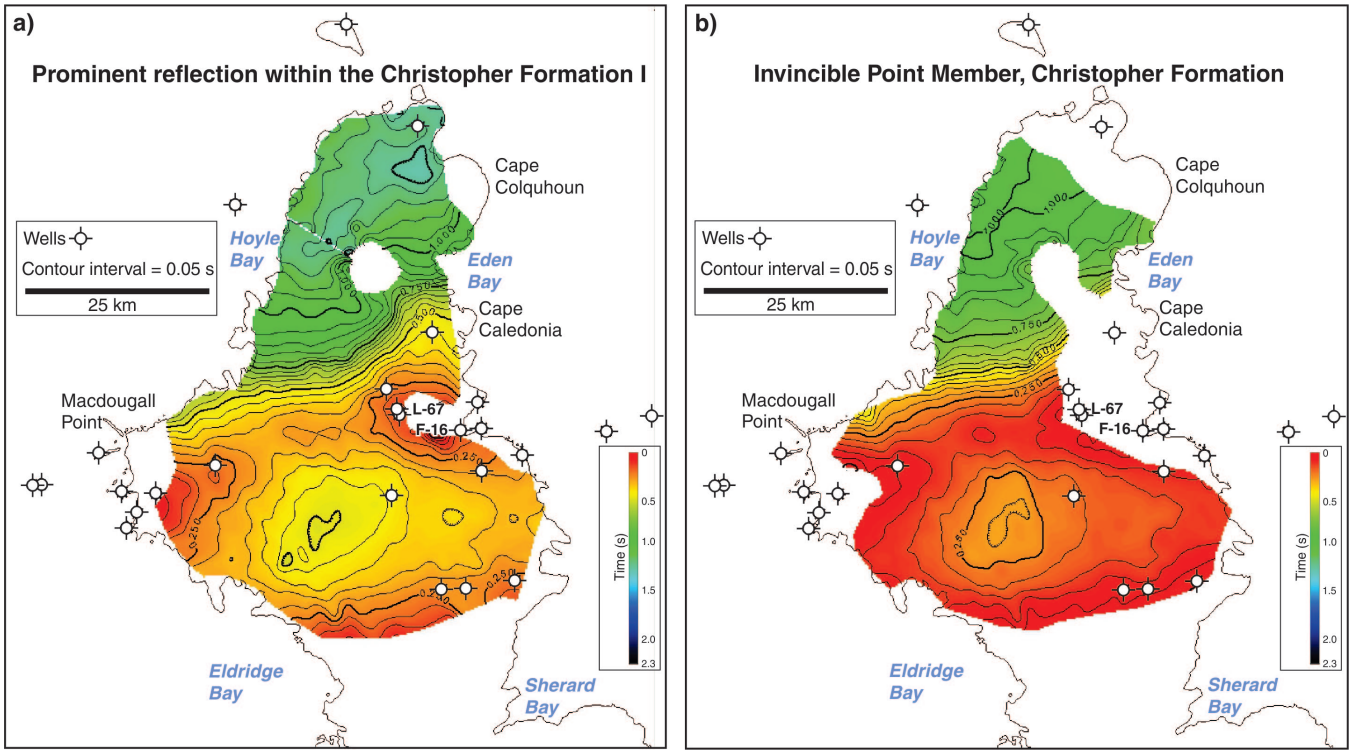

Figure 8. Time-structure maps of prominent reflections within the Christopher Formation identified within the shallow subsurface of Sabine Peninsula: **a)** Christopher Formation 1 and **b)** Invincible Point Member, Christopher Formation.

Invincible Point Member, Christopher Formation

Similar to the Christopher I time-structure map the Invincible Point map nearly reaches the surface and descends to a time-depth of 1.03 s (Fig. 8). The map emphasizes the fact that the reflection was too near the surface in the east of the peninsula to be correlated with certainty. Subtle changes are noted in the morphology of the depression and the linear flexure.

DISCUSSION

The structure maps of the six reflectors within the Mesozoic succession of the Sabine Peninsula indicate subtle changes in morphology with time. Overall the mapped reflections within the Mesozoic succession are nearly parallel to each other, resulting in a similar structure map for each. A quality that each of the reflections had in common was a slight loss of amplitude near the Drake L-67 well. The Drake well has a know presence of dry gas to which the attenuation in the area can be attributed.

Extensional faulting was noted throughout much of the data set spanning from the deeper section below the Gore Point reflection to the Christopher Formation I reflection. The offsets due to faulting were minor and did not impede seismic interpretation. The extensional faulting is interpreted to have occurred mainly in the Early Cretaceous, coincident with the opening of the adjacent Amerasia Basin and the emplacement of mafic dykes and sills in the Sabine Peninsula area (Balkwill and Fox, 1982). Later movements may have been coincident with the Eurekan Orogeny.

A prominent feature of the time-structure maps that remains relatively constant from the deepest Gore Point map up to the shallowest time-structure map of the Christopher Formation is the presence of the linear flexure spanning from Macdougall Point to Cape Caledonia. This feature is not preserved on modern topographic maps. Shallow re-processing of the best quality 2-D seismic lines (2000 series) indicates that the feature is in fact inherited from the deeper (possibly Permian) section. Furthermore, Late Carboniferous paleogeography indicates that the location of the linear flexure corresponds to the limit of a shallow carbonate shelf that covered the area (Embry and Beauchamp, 2008). According to the paleogeography model, the Sabine Peninsula was covered by fluvial to delta plains through much of the Triassic and by Late Jurassic consisted of shallow shelf sediments (Embry and Beauchamp, 2008). Given that the linear flexure appears to be inherited from the Permian or earlier topography, the flexure may in fact represent the limit of the Late Carboniferous shallow shelf from paleogeographic reconstructions.

The depression first noted on the Gore Point time-structure map gradually became isolated upward in the shallow succession. Structures controlling the boundaries of the depression are absent and only the continuous draped morphology is observed across the seismic data. In other words, there is no evidence of localized sediment deposits or small-scale erosional features either within the depression or across the data set. On seismic profiles the depression is gradual and the boundaries of the feature are not apparent. The depression is maintained throughout the shallow succession and interpreted as part of the Marryatt Point syncline described by Harrison (1995). Harrison stated that although the Upper Permian and younger rocks of the Sabine Peninsula are nearly flat-lying, broad folds are noted at the surface. The Marryatt Point syncline noted on the surface by Harrison (1995) coincides well with the depression location in the subsurface.

CONCLUSION

The preliminary results of shallow seismic reprocessing and seismic interpretation of onshore Sabine Peninsula yielded structure maps for six horizons within the Triassic through Cretaceous succession of the Sverdrup Basin.

Each of the time-structure maps displays subtle changes in the subsurface morphology. Two striking features are present on each time-structure map: 1) the flexure to the south of Barrow dome, and 2) the depression in the central part of the peninsula. The flexure represents the limit of the Late Carboniferous shallow carbonate shelf edge of the Sverdrup Basin inherited from the deeper section. The depression, on the other hand, represents the subsurface expression of the Marryatt Point syncline observed at the surface.

The structure of the Mesozoic horizons acts as a first approximation of the structure that can be expected for the deeper horizons as well as in the offshore. The deeper part of the succession is the target of the next phase of reprocessing and interpretation. Given the existing oil and gas discoveries in the vicinity, this type of information may guide exploration toward the identification of new hydrocarbon plays to be considered for resource assessment.

ACKNOWLEDGMENTS

This work was conducted through the Geo-mapping for Energy and Minerals (GEM) program of the Geological Survey of Canada (GSC). The Sabine Peninsula subsurface study is part of the GEM-Energy – Western Arctic Islands project. Suncor Energy is acknowledged for providing access to seismic data through the MOU. Special thanks are extended to GSC Calgary students for the quality control made on the original stacked sections. Thanks are also extended to K. Dewing and participants of the Western Arctic Islands project for valuable discussion. Thanks are extended to A. Embry (GSC Calgary) for reviewing an earlier version of this manuscript. IHS-Seismic Micro Technology is acknowledged for providing the seismic-interpretation software.

REFERENCES

Balkwill, H.R. and Fox, F.G., 1982. Incipient rift zone, western Sverdrup Basin; *in* Arctic geology and geophysics, (ed.) A.F. Embry and H.R. Balkwill; Canadian Society of Petroleum Geologists, Memoir 8, p. 171–187.

Brent, T.A., 2006. Seismic reflection interpretation of gas hydrates and permafrost in the High Arctic of Canada; *in* Proceedings of the Fourth International Conference on Arctic Margins, Dartmouth, Nova Scotia, September 30–October 3, 2003, U. S. Department of the Interior Minerals Management Service, 261 p.

Canales, L.L., 1984. Random noise reduction; *in* Expanded Abstracts, 54th Annual International Meeting, Society of Exploration Geophysicists, Session S10.1. p. 525–527.

Chilès, J.P. and Delfiner, P., 1999. Geostatistics: modeling spatial uncertainty; Wiley Series in Probability and Statistics, Wiley and Sons, New York, New York, 695 p.

Dewing, K. and Embry, A.F., 2007. Geological and geochemical data from the Canadian Arctic Islands. Part I: stratigraphic tops from Arctic Islands' oil and gas exploration boreholes; Geological Survey of Canada, Open File 5442, 1 CD-ROM. doi:10.4095/223386

Dewing, K. and Obermajer, M., 2011. Chaper 38. Thermal maturity of The Sverdrup Basin, Arctic Canada and its bearing on hydrocarbon potential; Geological Society; Memoir, v. 35, p. 567–580.

Dunbar, M. and Greenaway, K.R., 1956. Arctic Canada from the Air; Canada Defense Research Board, Queen's Printer, Ottawa, Ontario, 541 p.

Embry, A.F., 1984a. Stratigraphic subdivision of the Roche Point, Hoyle Bay and Barrow Formations (Schei Point Group), Western Sverdrup Basin, Arctic Islands; *in* Current Research, Part B; Geological Survey of Canada, Paper 84-1B, p. 275–283. doi:10.4095/119583

Embry, A.F., 1984b. The Wilkie Point Group (Lower-Upper Jurassic), Sverdrup Basin, Arctic Islands; *in* Current Research, Part B; Geological Survey of Canada, Paper 84-1B, p. 299–308. doi:10.4095/119585

Embry, A. and Beauchamp, B., 2008. Sverdrup Basin; *in* Sedimentary basins of the world, (ed.) K.J. Hsü; Volume 5, The sedimentary basins of the United States and Canada, Elsevier, Amsterdam, The Netherlands, p. 451–471.

Embry, A.F. and Johannessen, E.P., 1992. T-R sequence stratigraphy, facies analysis and reservoir distribution in the uppermost Triassic-Lower Jurassic succession, western Sverdrup Basin, Arctic Canada; *in* Arctic geology and petroleum potential, (ed.) T.O. Vorren, E. Bergsager, Ø.A. Dahl-Stamnes, E. Holter, B. Johansen, E. Lie, and T.B. Lund; Norwegian Petroleum Society (NPF), Special Publication 2, p. 121–146.

Goodbody, Q.H. and Christie, R.L., 1993. Summary of stratigraphy of Melville Island, Arctic Canada; *in* The Geology of Melville Island, Arctic Canada, (ed.) R.L. Christie and N.J. McMillan; Geological Survey of Canada, Bulletin 450, p. 13–22.

Greenaway, K.R. and Colthorpe, S.E., 1948. An aerial reconnaissance of Arctic North America; Joint Intelligence Bureau, Ottawa, Ontario, 300 p.

Harrison, J.C., 1995. Melville Island's salt-based fold belt, Arctic Canada; Geological Survey of Canada, Bulletin 472, 344 p.

Lindseth, R.O., 1979. Synthetic sonic logs - a process for stratigraphic interpretation; Geophysics, v. 44, p. 3–26. doi:10.1190/1.1440922

Marfurt, K.J., Scheet, R.M., Sharp, J.A., and Harper, M.G., 1998. Suppression of acquisition footprint for seismic sequence attribute mapping; Geophysics, v. 63, p. 1024–1035. doi:10.1190/1.1444380

Matheney, M.P. and Nowack, R.L., 1995. Seismic attenuation values obtained from instantaneous-frequency matching and spectral ratios; Geophysical Journal International, v. 123, p. 1–15. doi:10.1111/j.1365-246X.1995.tb06658.x

Merritt, R.K., 1974. Seismic reflection measurements in the Canadian Arctic Islands; *in* Proceedings of the 1973 National Canadian Society of Exploration Geophysicists Convention, Calgary, Alberta, April 4–6, 1973, p. 89–105.

Sengbush, R.L., Lawrence, P.L., and McDonal, F.J., 1961. Interpretation of synthetic seismograms; Geophysics, v. 26, p. 138–157. doi:10.1190/1.1438851

Stephenson, R.A., Van Berkel, J.T., and Cloetingh, S.A.P.L., 1992. Relation between salt diapirism and the tectonic history of the Sverdrup Basin, Arctic Canada; Canadian Journal of Earth Sciences, v. 29, p. 2695–2705. doi:10.1139/e92-213

Waylett, D.C., 1990. Drake Point Gas Field, Canadian Arctic Islands; *in* Structural traps; I. Tectonic fold traps, (ed.) E.A. Beaumont and N.H. Foster; American Association of Petroleum Geology, Treatise of Petroleum Geology, Atlas of Oil and Gas Fields A-016, p. 77–102.

Geological Survey of Canada Project EGM004